https://doi.org/10.59531/ots.2025.3.2.115-144

APPLICATION OF GEOPHYSICAL METHODS TO THE ASSESSMENT OF ENVIRONMENTAL VULNERABILITY OF URBAN AREAS

[VÁROSI TERÜLETEK KÖRNYEZETI SÉRÜLÉKENYSÉGÉNEK ÉRTÉKELÉSE GEOFIZIKAI MÓDSZEREK ALKALMAZÁSÁVAL]

ZSUZSANNA PLANK[1*], ZSOLT PRONAY[2]

[1]Multidisciplinary Ecotheolgical Research Institute, John Wesley Theological College; Danko utca 11 Budapest, 1086 Hungary,

https://orcid.org/0000-0001-8466-5090

*corresponding author: plankzsu@gmail.com

[2] Mingeo Ltd., Ráskai Lea u. 20. Budapest 1142 Hungary

https://orcid.org/0000-0003-2266-8987

Abstract. The pluvial flood hazard of an urban area can be characterized by the environmental vulnerability. It is a measure that depends on three spatial factors: morphology, water coverage and the drainage capacity of the ground. Since the drainage capacity is the function of the composition and structure of the overburden layers, geophysical survey data can assist in the assessment of flood hazard.We worked out a methodology for determination the high-resolution distribution of environmental vulnerability using data from two geophysical surveying methods that are applicable in urban areas. In case of the ground penetrating radar method, the surface drainage capacity was linked to the clay content of the overburden. Thus, the attenuation of the electromagnetic waves could be correlated with the permeability factor of the environmental vulnerability. When relating this factor to the data of a DC electric survey we correlated the electrical resistivity values to the dominant grain size distribution of the upper layer. We demonstrate the application of this methodology in two urban field studies in Hungary, where the environmental vulnerability was defined along geophysical survey lines with horizontal resolution of the surveying method. In the first case, GPR method was used to determine the permeability factor and a digital terrain model served as the source of morphology data. The second case was in a flat area, where there was no need for slope data. The permeability factor was derived from electrical resistivity values of a three km long survey line and grain size analysis results of drill.

Keywords: pluvial flood hazard, vulnerability index, attenuation of GPR waves, DC resistivity survey, water-permeability

https://doi.org/10.59531/ots.2025.3.2.115-144

Introduction

Pluvial floods may occur frequently in urban areas as one among the harmful consequences of global climate change. Bueno et al (2012) showed that the impact assessment of pluvial floods requires the involvement of several fields of sciences (Geotechnics, Environmental Sciences, Economics, Social Sciences). Indexing the environmental vulnerability, the terrain and geological conditions affecting the surface water drainage can be quantified.

Rotárné at al. (2016) worked out a methodology for determination of vulnerability of subsurface aquifers. The following tasks were performed during the impact assessment:

- Making aerial photos for determination of surface coverage
- Preparing high resolution Digital Terrain Model
- Preparing the surface flow model of the area
- Defining the exposure indicator
- Surface geophysical survey and shallow drill sampling for high resolution imaging of the aquifer
- Integrated interpretation of acquired data
- Impact assessment

Plank at al (2016) presented the application of this vulnerability assessment method in a test site.

The environmental risk assessment method approved by the Intergovernmental Panel on Climate Change (IPCC) of the European Union (IPCC 2014) defines the climate risk as the function of three pillars: hazard, exposure and vulnerability (V).

The environmental vulnerability of near surface structures is directly connected to the dominant grain size range of the overburden, which can be derived from the results of various geophysical surveying methods. Kirsch et al (2003) used large scale mapping of electromagnetic conductivity to define the vulnerability index that reflects the territorial exposure of aquifers against pollution. Christensen and Christiansen (2021) demonstrated the vulnerability of an aquifer with the thickness of a clay overburden defined through electromagnetic survey data. Obiora et al. (2016) used interpretation of geoelectric mapping for aquifer delineation and vulnerability determination.

Dannowski and Yaramanci (1999) demonstrated in a field example that it is worth combining ground penetrating radar (GPR) and geoelectric resistivity methods for

https://doi.org/10.59531/ots.2025.3.2.115-144

defining the physical parameters of a porous media. Using GPR huge amount of high-resolution data can be acquired in relatively short time. The shielded antennas can be used even in urban environment; consequently, GPR survey is an effective tool in defining the distribution of vulnerability. Ground penetration radar method is appropriate for investigating shallow sediments in urban areas as it was shown in field experiments by Słowik (2014).

According to Lunt et al (2005) the climatic conditions have significant influence on the attenuation of GPR waves in near surface environment. Besides the surveying frequency, the penetration depth of electromagnetic waves is the function of the dielectric properties of the investigated medium as it depends on the hydrogeological parameters such as clay content, porosity, grain size distribution (Boll et al. 1996; Neal 2004; Steelman and Endres 2010). According to Daniels, 2004 the layer's clay content has the major impact on attenuation of the electromagnetic waves in the frequency range over 50MHz . Wunderlich and Rabbel, (2013) directly linked the frequency change and attenuation loss of the reflected GPR signals to the clay and water content of the examined soil samples

In general, the electrical resistivity of sediments depends on grain size, degree of saturation, and the resistivity of the fluid in the soil pores (Smith and Sjorgen 2006). Furthermore, the electrical potential formed on the surfaces of the clay particles lowers the resistivity of the layers with dominant clay content (Hou et al. 2009).

The purpose of this study is to show a scientifically based indexing method for indexing environmental vulnerability even in urban/built in areas. The geophysical field survey is the key point of the method because it provides data with high areal resolution. Since the problem of pluvial floods affects built in areas we were focusing on involving such geophysical survey methods that can be reliable applied even in urban areas where -compared to rural field conditions- there are specific challenges to keep the signal/noise ratio at an acceptable low level.

Methodology

Vulnerability calculation

Sperotto et al. (2016) introduced a physical and environmental vulnerability assessment method for giving the territorial pluvial flood risk considering the near surface geological composition. They define the environmental vulnerability as the function of three factors: slopes (f1), water permeability (f2) and water coverage (f3).

https://doi.org/10.59531/ots.2025.3.2.115-144

Each factor can take a value between 1 (very vulnerable) and 0 (not vulnerable). The vulnerability pillar can be calculated with Formula (1):

$$V = \otimes_{i=1}^{3} f_i \quad (1)$$

where the symbol ⊗ indicates the operator „probability or ", given by Kalbfleisch (1985).

For determination of slope factor (f1) application of high-resolution digital terrain model is recommended however, in smaller sites, surface geodesy can be also appropriate. The effect of the soil permeability appears at factor f2. It is quantified upon the clay content of the overburden based on the soil's grain size distribution. The f2 value in built up areas equals one. For the values of the surface coverage factor (f_3) the value of 0.8 is given if there is water on the surface and 0.2 in case of a dry surface.

Converting physical parameters such as slope or water permeability into dimension free vulnerability factor is a useful tool to be able to express environmental vulnerability with a single number that still represents the parameters that it was derived from. Figure 1 illustrates the three factors and the derived vulnerability using the Kalbfleisch operator in some theoretical cases. It can be observed, that due to the mathematical characteristics of the Kalbfleisch operator, the vulnerability value is always higher that the highest factor value, no matter how low the other factors are. Furthermore, if any of the three factors equals one, it makes the vulnerability to 1.

https://doi.org/10.59531/ots.2025.3.2.115-144

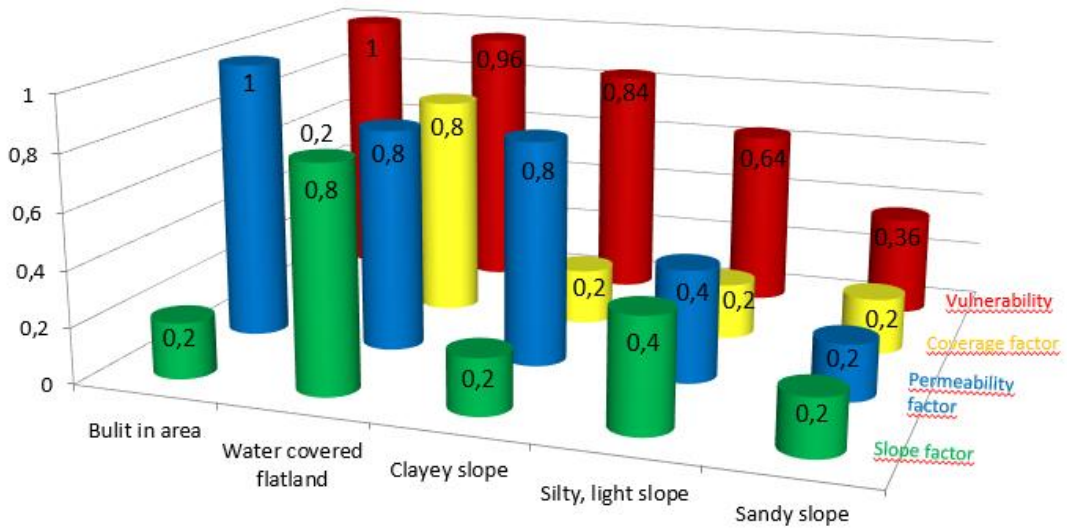

***Figure 1**.: Environmental vulnerability values calculated from the factors of slope, permeability and surface coverage after Sperotto at al (2016). [A lejtés-, áteresztőképesség- és felszínborítás faktorokból számított környezeti sérülékenység értékek Sperotto at al (2016) alapján]*

Sperotto at al. (2016) defined the permeability factor upon the correlation between water infiltration capacity and clay content (Table 1).

https://doi.org/10.59531/ots.2025.3.2.115-144

***Table 1**. Clay content, layer permeability and vulnerability factor values after Sperotto at al. (2016) [Agyagtartalom, a réteg áteresztő képessége és a környezeti sérülékenység értékek Sperotto at al (2016) alapján]*

Layer description	**Permeability**	**Permeability factor f_2**
Stratified clay	$<10e^{-8}$ m/s	0,8
Clay with silt	$10e^{-8} – 10e^{-7}$ m/s	0,6
Silt	$10e^{-7} – 10e^{-6}$ m/s	0,4
Fine sand	$10e^{-6} – 10e^{-5}$ m/s	0,3
Sand and gravel	$>10e^{-5}$ m/s	0,2

Determination of permeability factor from geophysical data

The DC (direct current) electrical resistivity and the propagation of electromagnetic waves are both physical parameters that depend on certain hydrogeological parameters (i.e., clay content, porosity, dominant grain size) of the investigated medium. Consequently, they can be used for determination of the permeability factor.

From the point of vulnerability assessment against pluvial flooding only the permeability of the surface layer is relevant, which is evidently located over the ground water table in case of dry surface coverage. With the lack of pore fluid in the unsaturated zone the resistivity dominantly depends on the clay content. Once the attenuation loss of the GPR waves is a direct indicator of the layer's clay content, it can be linked to the permeability of the overburden. For this purpose, we introduced the parameter D10 representing the depth where the amplitude of the direct, high frequency electromagnetic wave decreases to its 10%. With other words: D10 is the depth where the attenuation loss of the GPR wave reaches 90%. It means that the higher the clay content of the upper layer, the higher the attenuation loss, the lower the D10 depth. From the other point of view higher clay content is linked to less water infiltration capacity, which means higher vulnerability for a pluvial flood.

By measuring the DC resistivity of the surface layer using geoelectric surveying methods combined with grain size analysis of soil samples, the permeability factors can be derived along the survey line. First the correlation between the physical properties such as electrical resistivity and geological parameters affecting water

https://doi.org/10.59531/ots.2025.3.2.115-144

infiltration such as grain size distribution need be set up with the combined interpretation of geoelectric surveying data and drill hole sample analytics. Next, the permeability factor can be linked to the electrical resistivity as presented in Table 1.

Field study 1

This field study presents the application of GPR method in determination of surface vulnerability. The test site was in a village in the valley of River Sárvíz in central Hungary. The assessment of the area from the point of environmental vulnerability may be useful for development of a new water management plant and may strengthen the local decision makers' commitment for implementing local adaptation measures. The region of the investigated site is part of a system with living waters, fishponds, channels, marshes, with a unique birdlife and freshwater habitats, excellent possibilities for fish farming, angling and soft tourism. Permanently dry areas are covered with good quality soil (high organic matter content, high permeability) being used for intensive agriculture.

Site characterization

The near surface geological structure of site was reconstructed after the data of several shallow bore holes (maximal depth of 50m), GPR and geoelectric surveys. The location map of the investigated area is shown in Figure 2.

https://doi.org/10.59531/ots.2025.3.2.115-144

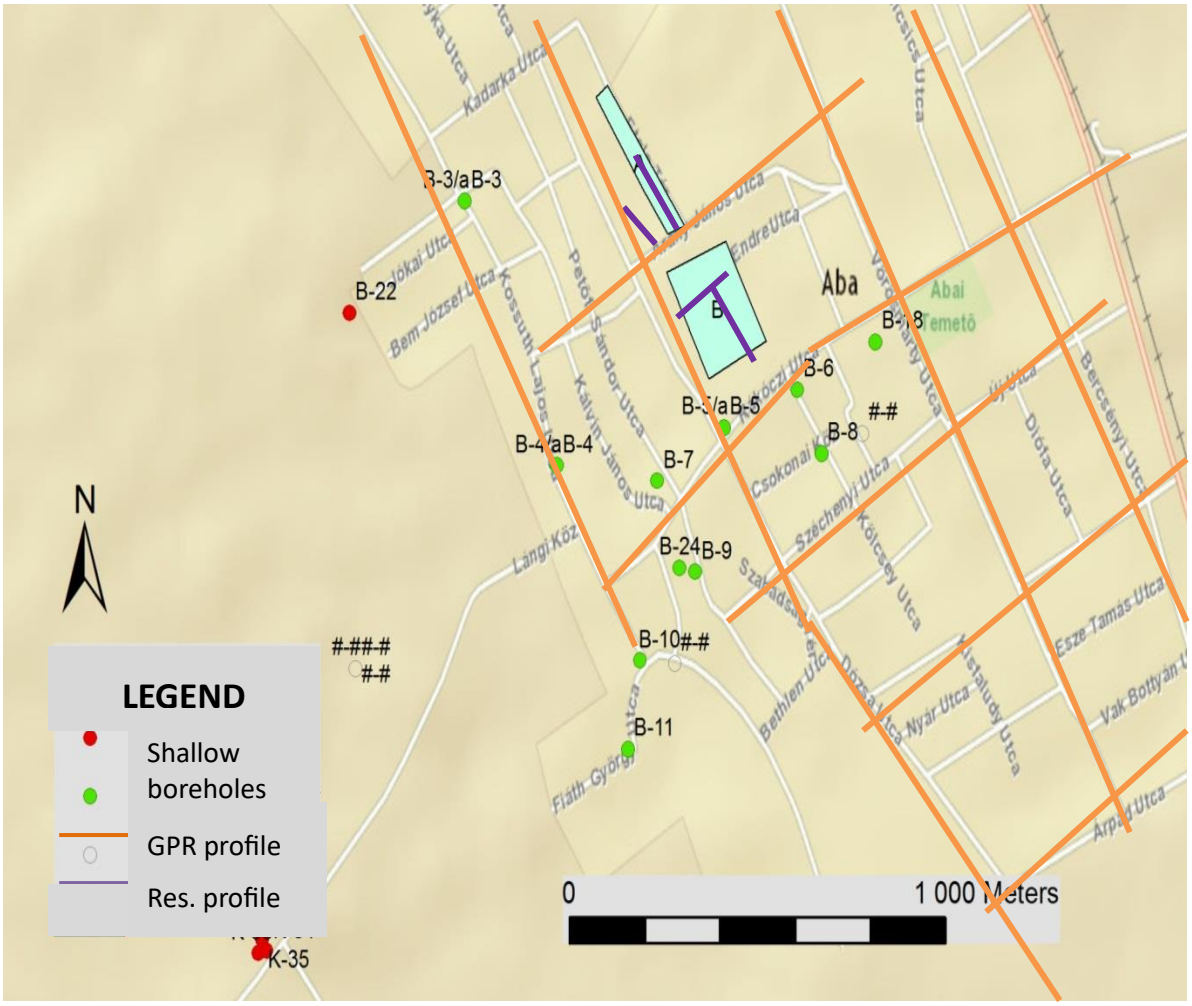

Figure 2.: *Location map of the investigated site. [A kutatási terület helyszínrajza]*

The geological structure reflects to conventional alluvial sedimentation: layers with various clay and sand content. A typical geological sequence is presented in Table 2. From the point of vulnerability against intense rainfall the zones with low water permeability indicated by high clay content may be dangerous.

https://doi.org/10.59531/ots.2025.3.2.115-144

Table 2. *Typical drill hole sequence. [Tipikus fúrási rétegsor.]*

Depth from (m)	**to** (m)	**Thickness (m)**	**Layer content**
0	2	2	Soil
2	2.6	0.6	silty sand
2.6	4.7	2.1	sandy clay
4.7	25.9	21.2	marl
25.9	34	8.1	sand
34	43.8	9.8	silty sand
43.8	45	1.2	clay

The GPR data acquisition was carried out along 17 survey lines using SIR-20 equipment with 200 MHz, shielded antennas. Table 2. gives the technical details of the GPR profiles.

Table 3. *Technical parameters of GPR survey lines. [A földradar mérési vonalak műszaki paraméterei.]*

Line number	**Length**	**Number of channels**
2	97 m	974
3	530 m	5326
4	715 m	5134
5	2159 m	53886
6	1909 m	41598
7	1561 m	20510
8	1130 m	21358

https://doi.org/10.59531/ots.2025.3.2.115-144

9	705 m	19902
10	459 m	8366
11	1875 m	33966
12	583 m	13262
13	457 m	10110
14	498 m	12238
15	104 m	1038
16	2248 m	24622
17	310 m	3054
Total:	15340 m	275344

After digital signal processing (background removal with f-k filtering and automatic gain control) 0.1 m/ns average propagation velocity was used for depth transformation. Figure 3 presents a 300 m long, typical GPR profile after this processing step. Red arrows indicate a layer boundary in the depth range of 1.6-2.0 m. This boundary cannot be detected in the left side of the radargram due to the attenuation loss cause by increasing clay content. Such zones were identified as locations vulnerable to flooding.

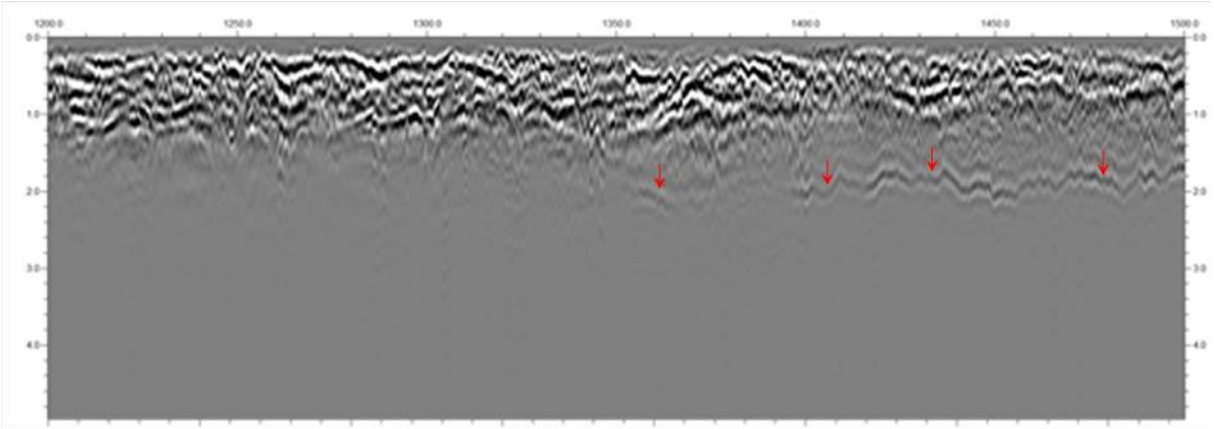

Figure 3*.Sample GPR profile in the investigated site. Red arrows indicate a layer boundary. [Példa földradal szelvényre a vizsgált területről. A piros nyilak jelzik a réteghatárt.]*

https://doi.org/10.59531/ots.2025.3.2.115-144

Geoelectric resistivity survey was done along 4 profiles in order to get detailed information on the endangered zones having been marked upon the GPR results of investigations. The measurements were carried out with a Syscal Junior multi-electrode system using 72 electrodes in a roll-along array introduced by Dahlin and Bernstone (1997). Based on the studies of Plank and Polgár (2019) a Wenner-Schlumberger electrode configuration was used with a 2 m unit electrode distance in order to image the resistivity distribution of the upper 20 m. The data processing was done using a Gauss-Newton method developed by Loke and Barker (1996). The resistivity values were linked to geological layer information using the drill hole data. One interpreted profile is shown in Figure 4. Below a thin, resistive soil overburden there is a clay layer that can be characterized with resistivity values lower than 15 Ohmm. Below there is a saturated sand layer (resistivity over 25 Ohm) with some silt intercalations (20-25 Ohmm).

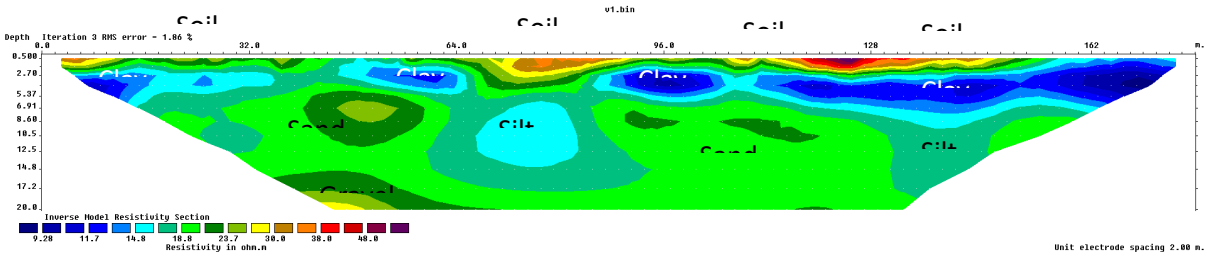

***Figure 4**.: Interpretaed typical resisitivity profile. The colour scale indicates the resistivity values in Ohmm. [Egy tipikus fajlagos ellenállás szelvény értelmezés után. A színskála a fajlagos ellenállás értékeket jeleníti meg ohmméterben.]*

Determination of vulnerability factors

A high resolution, digital terrain model (DTM) of the site was set up based on the data of an air borne geodesy survey. From the DTM high resolution slope values and directions were derived.

According to the instructions of Sperotto et al (2016) the slope values were linked to one the three possible slope factor values. The flat area gets the factor value of 0.8 while the steepest part with the slope over 10.27% gets 0.2.

https://doi.org/10.59531/ots.2025.3.2.115-144

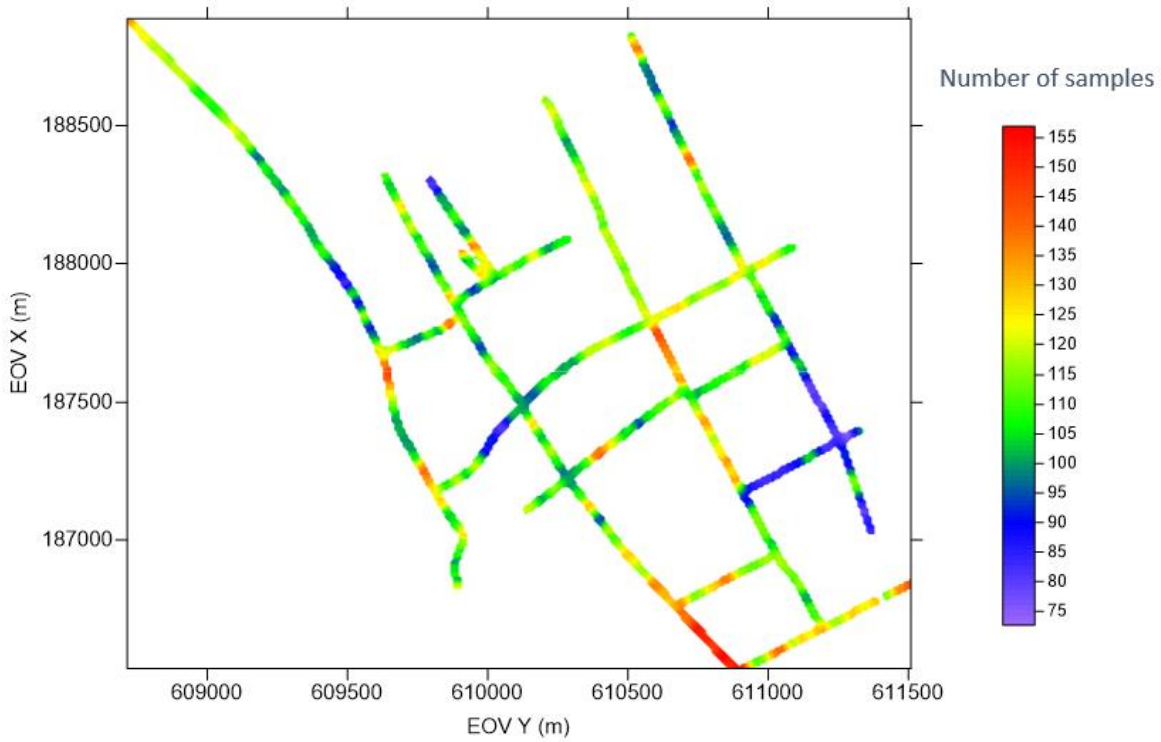

The permeability factor was calculated from parameter D_{10} representing the attenuation loss in the top layer due to its clay content. At the first stage of the calculation the number of samples in the received signals were counted until the signal lost 90% of its amplitude. This calculation was done for each channel of all survey lines as shown in Figure 5.

Next the depth scale was set using the wave propagation velocity of 0.1 ns/m. As a result, for example, 75 samples before losing 90% of the initial signal represented 0.36 m of D_{10} depth, while 155 samples 0.78 m. Following Sperotto's permeability classifications the f_2 factor was defined upon the D_{10} depth as given in Table 4.

***Table 4**. Layer characteristices linked to D_{10} depth and vulnerability factor values [Rétegjellemzők hozzárendelése D_{10} mélységhez és a környezeti sérülékenység értékekhez]*

Layer description	**D_{10} range**	**Permeability factor f_2**
pure layered clay	0-0,25 m	0,8

https://doi.org/10.59531/ots.2025.3.2.115-144

clay with silt	0,251-0,35 m	0,6
silt	0,351-0,5 m	0,4
fine sand	0,51-0,75 m	0,3
sand and gravel	over 0,75 m	0,2

Finally, the factor for surface coverage was determined upon the photos of the air borne survey.

Vulnerability assessment

For demonstrating the applicability of the vulnerability assessment method based on GPR survey we chose two GPR profiles in the area that were classified as *endangered* upon the DTM. Figure 6 shows a DTM cut off with the locations of the chosen survey

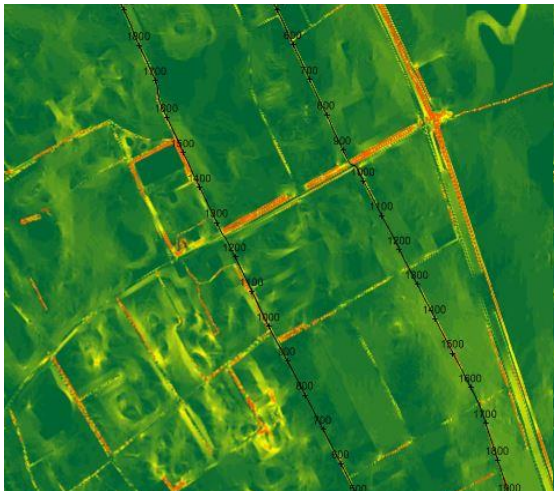

Figure 5. *Digital terrain model with the traces of the GPR profiles. [Digitális felszínmodell és a földradar mérési szelvények nyomvonalai.]*

lines (drawn in black). The dark green zones indicate flat areas, while the orange and red ones refer to increasing slope.

Figure 7 shows the calculated slope and permeability factors along the two survey lines.

https://doi.org/10.59531/ots.2025.3.2.115-144

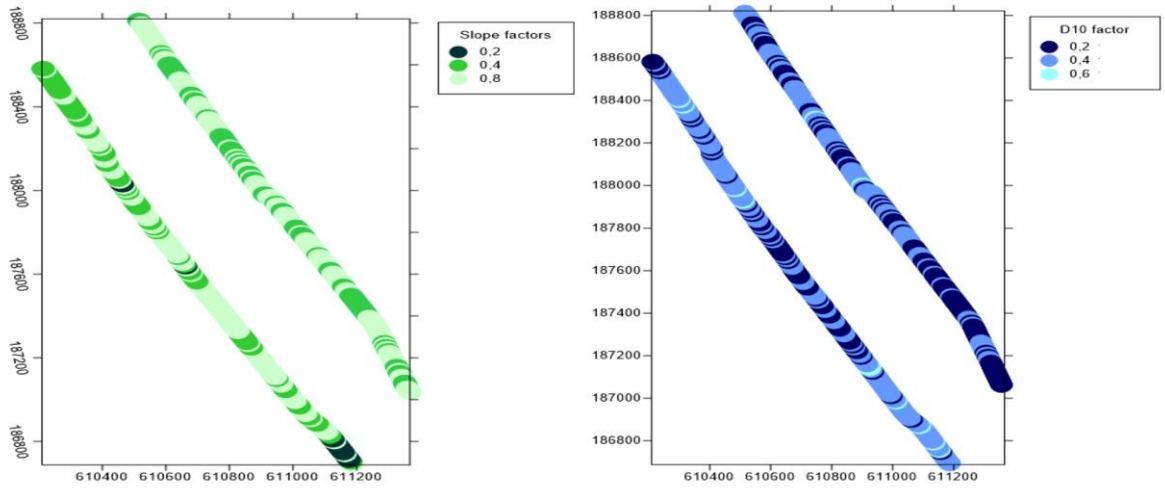

Figure 6. *Slope factor (green) and permeability factor (blue). [Lejtésfaktor (zöld) és áteresztőképesség faktor (blue).]*

The factor f_3 was defined upon the delineated water coverage. The traces of the GPR profiles were in dry areas with the uniform f_3 value of 0.2. The environmental vulnerability was calculated upon the three factors using the Kalbfleisch operator from point by point along the GPR profiles as it is shown in Figure 8. The dark red zones indicate areas with extremely high vulnerability due to the combination of flatness and low water permeability of the near surface overburden. The areas with medium vulnerable against pluvial floods are marked with yellow. Here the higher water drainage capacity decreases the vulnerability due to the combination of dipping surface and lower clay content in the near surface region.

https://doi.org/10.59531/ots.2025.3.2.115-144

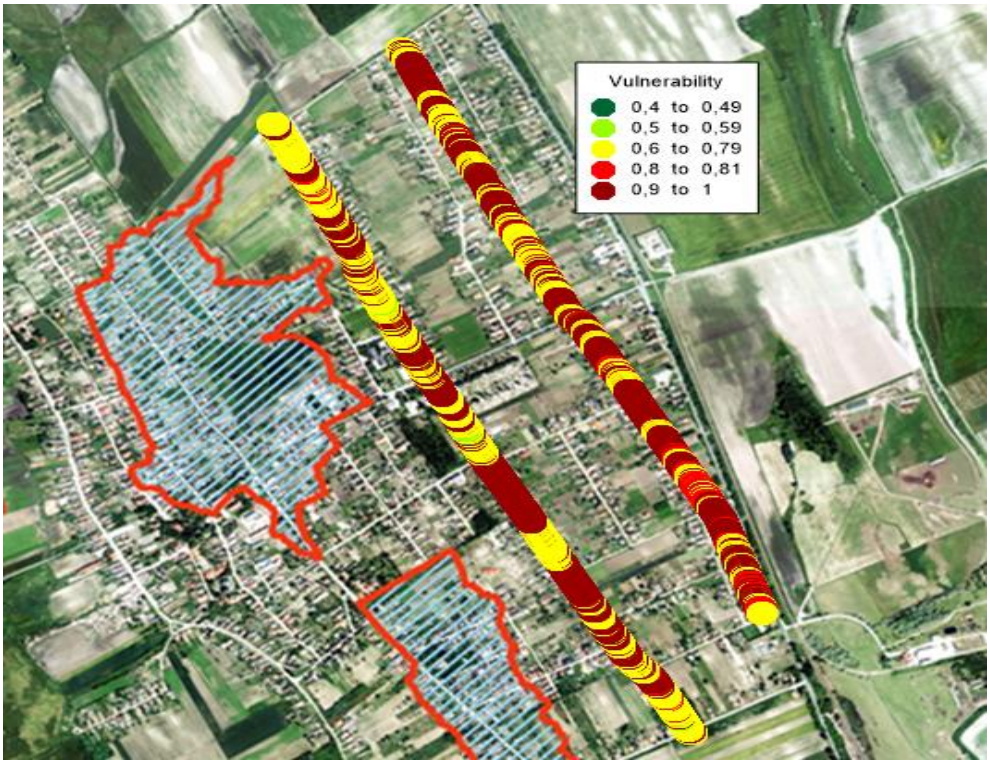

***Figure 7**. Environmental vulnerability along two GPR profiles. The darker red the circles the higher the vulnerability.[Környezeti sérülékenység két földradar szelvény mentén. A sötétebb vörös árnyalatú körök magasabb sérülékenységet jeleznek.]*

Discussion to Field study 1

In this field study we presented the elaboration of vulnerability indexing method based on ground penetration radar data. Previously this site has been qualified the method based on the high-resolution data of a DTM described by Rotárné (2016). As a result of this previous survey endangered zones were marked (striped areas in Fig 8.). In our vulnerability indexing method we related the water permeability characteristics of the earth with the attenuation of the electromagnetic waves. Applying our GPR-based indexing we could improve the areal resolution of the geological factor besides the slope factor of the terrain model. As a result, the areal resolution of marking the

https://doi.org/10.59531/ots.2025.3.2.115-144

endangered sites were increased: in Figure 8 the heavily endangered zones are marked with dark red dots.

https://doi.org/10.59531/ots.2025.3.2.115-144

Field study 2

The site for demonstrating the derivation the permeability factor from geoelectric resistivity data is located in a suburban district of the capital, Budapest. It is at the bank of a regulated branch of the River Danube in the northern part of an island named Csepel. The site is built up from fluvial sediments: sandy-gravel layers with silt and clay intercalations. The overburden is a thin upfill material. The investigated site is a 3 km long flatland in a protected green zone that is few hundred meters wide between the river branch and urban area. Due to a sluice cutting off the river branch from the main water flow, the fluctuation of the water level is under control and does not depend on weather conditions. Thus, the area is highly endangered by pluvial floods as shown in the photos in Figure 9.

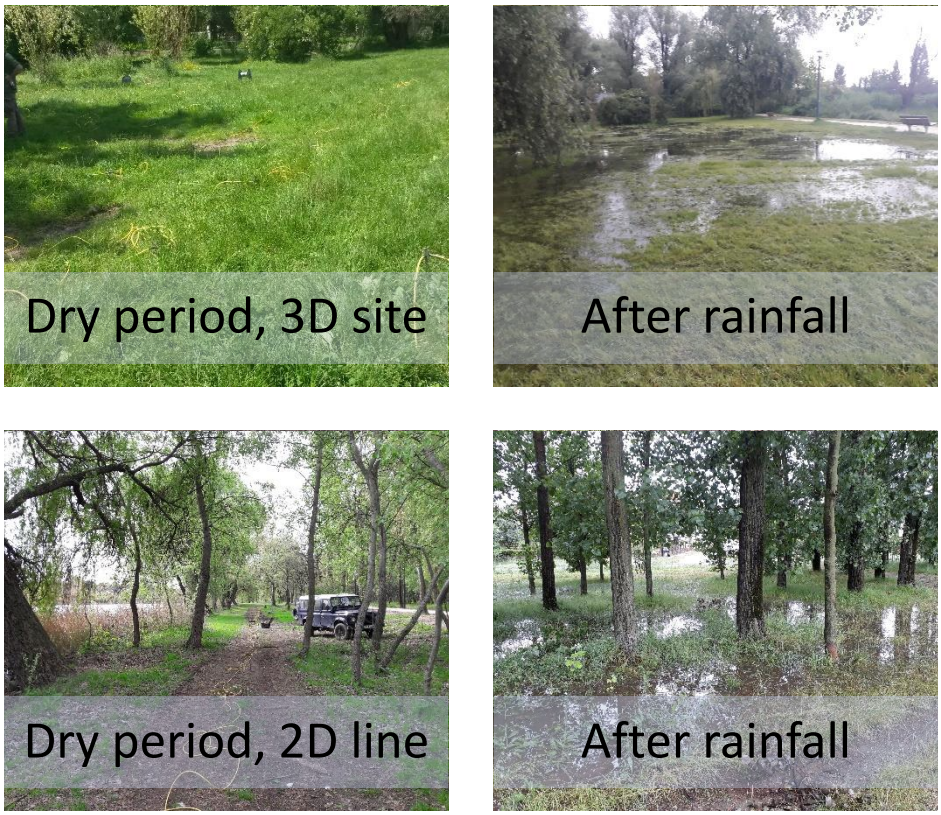

***Figure 8**.: Photos in the investigated area in dry weather and after rainfall. [A kutatási területről készült fényképek száraz időszakban és esőzés után.]*

https://doi.org/10.59531/ots.2025.3.2.115-144

Site characterization

The near surface geological structure of the investigated area was reconstructed after geoelectric resistivity data. Two survey campaigns were done: once a nearly 3.2 km long survey line along the riverbank was measured with an inverse Schlumberger array using the roll-along technique with the ABEM Swift String 8R instrument. The unit electrode distance was 2.5 m, the number of depth levels was: n=11. Secondly a 3D resistivity survey was carried out with 72 electrodes in a pole-pole array separated to 2 m unit distance. Figure 10 shows the location map of the field activities, while the details of the applied 2D and 3D arrays are given by Loke, 2015.

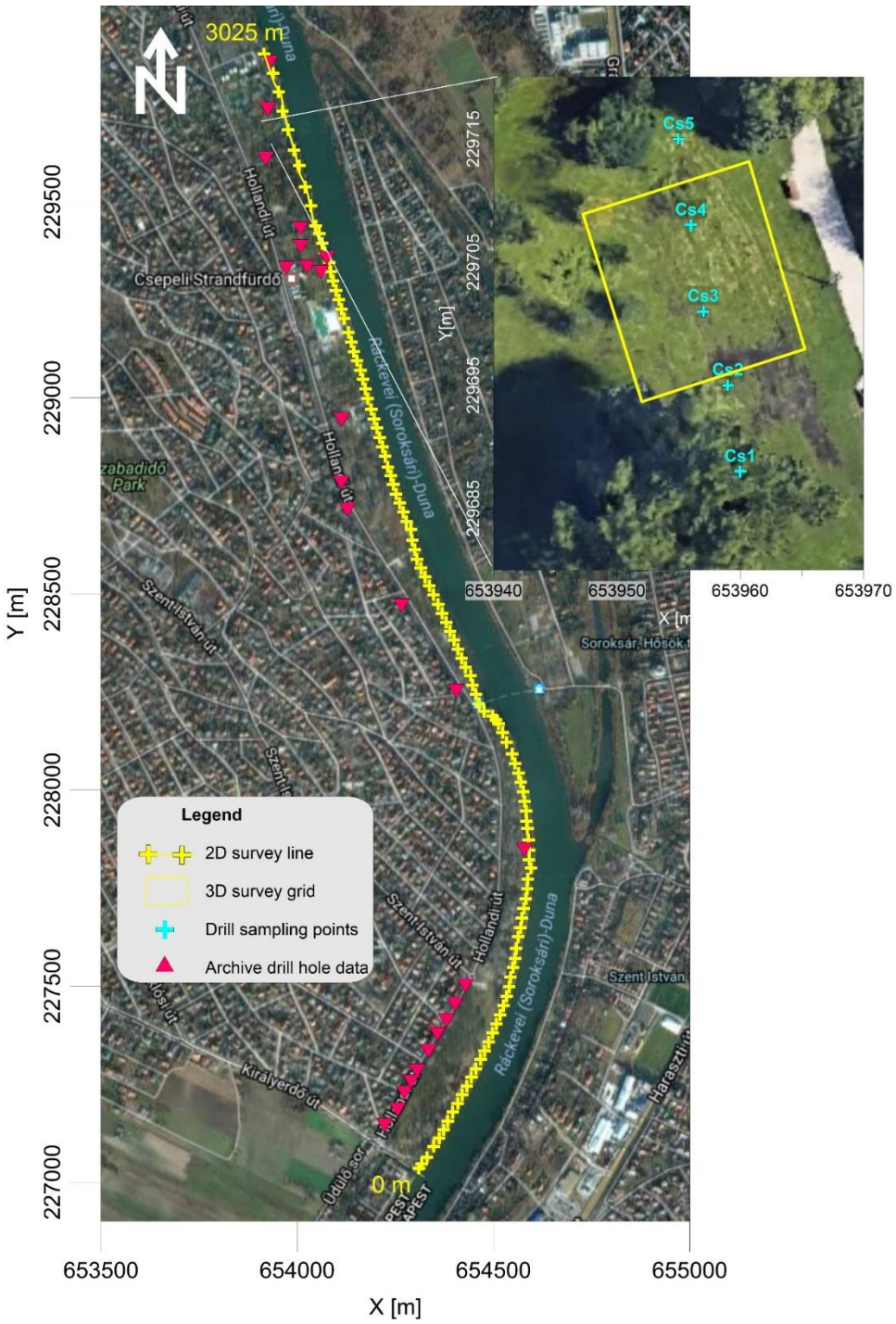
3025 m
0 m
Cs5
Cs4
Cs3
Cs2
Cs1
229715
229705
229695
229685
Y [m]
653940
653950
653960
653970
X [m]
229500
229000
228500
228000
227500
227000
Y [m]
653500
654000
654500
655000
X [m]
Csepeli Strandfürdő
Holland út
Rackevei (Soroksári) Duna
Szent István út
Soroksár, Hősök
Szent István
Királyerdő út
Legend
2D survey line
3D survey grid
Drill sampling points
Archive drill hole data

https://doi.org/10.59531/ots.2025.3.2.115-144

***Figure 9**. Location map of the investigated site. [A kutatási terület helyszínrajza.]*

The data processing was done with the software Res2Dinv and Res3Dinv. The geological interpretation was done using archive borehole data and the results of soil sample analysis. Figure 10 show the location map of the site with the survey lines and drill hole positions. According to the 2D resistivity profile there is a remarkable resistivity variation in the near surface overburden. The typical resistivity value is in the range of 16-30 Ohmm at first 1000 m of the profile representing wet soil with high clay content. From the middle part of the profile the clayey overburden is substituted by soil with mixed construction material with large grain size and low clay content. The typical resistivity increases to over 80 Ohmm. The lower layer consists of typical fluvial sediments with various grain size distribution: gravel (60-80 Ohmm), coarse sand (60-40 Ohmm), fine sand (30-40 Ohmm), aleurit (20-30 Ohmm). The bottom layer is a conductive aleurit with high clay content (the resistivity is below 20 Ohmm). Figure 11 shows some sample sections of the 2D resistivity profile with its geological interpretation.

https://doi.org/10.59531/ots.2025.3.2.115-144

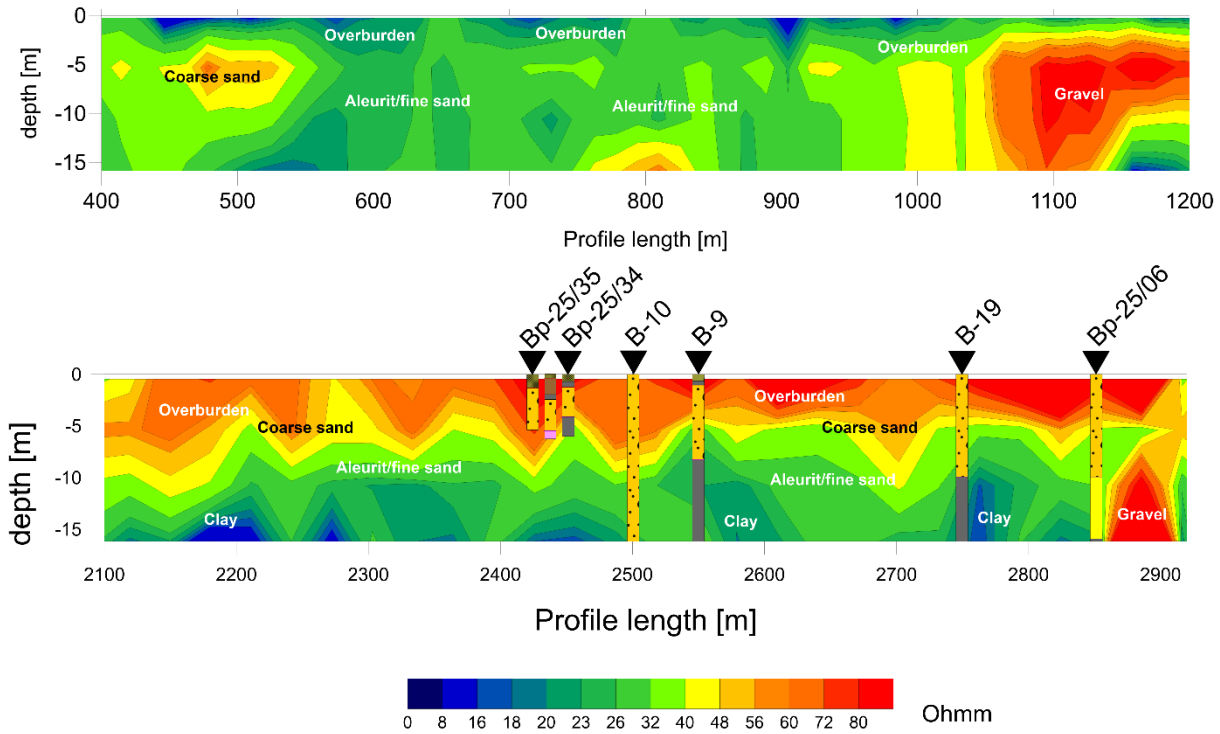

***Figure 10**. Sections of the 2D resistivity profile with bore hole information and geological interpretation. [2D Fajlagos ellenállás szelvenyek fúrólyuk adatokkal és földtani értelmezéssel.]*

The 3D resistivity survey combined with shallow drill hole sampling provides a reliable and high-resolution image of the geologic structure of the upper 18 m (Figure 12). The thin overburden is a conductive Holocene layer with high clay content. It is bordered by a resistive layer with large sized particles, that is identified as Pleistocene sand and gravel. The lowest layer is an upper Miocene, conductive aleurit with high clay content.

https://doi.org/10.59531/ots.2025.3.2.115-144

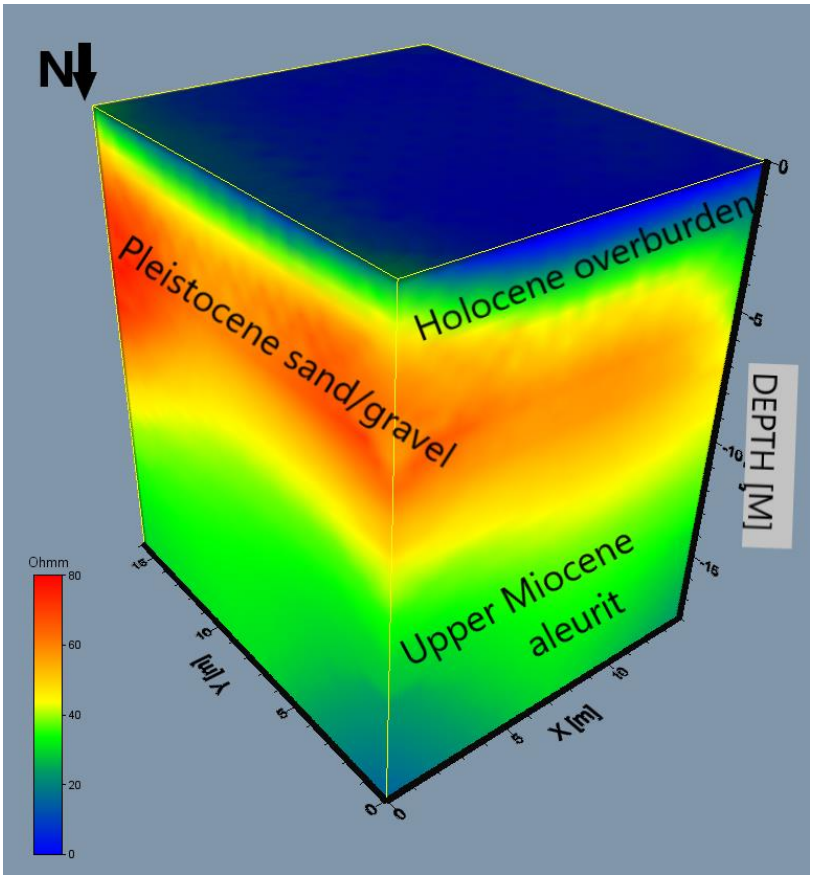

***Figure 11**.: Geological interpretation of the 3D resistivity survey. [3D fajlagos ellenállás mérés földtani értelmezése.]*

Determination of permeability factor

For determination of the permeability factor the results of the laboratory soil sample analytics were correlated with the 3D resistivity survey. We took the variations of the grain size distribution of the drill hole samples corresponding to the parameters in Table 1. At the next step we took the electrical resistivity value of the horizontal and vertical reference points nearest the sediment sample location and matched them to the dominant grain size fractions. Figure 13 shows the typical the grain size distribution and electrical resistivity values for the different permeability factors.

Finally, we defined ranges of electrical resistivity for all each grain size category by setting up confidential intervals a shown in Table 5.

https://doi.org/10.59531/ots.2025.3.2.115-144

https://doi.org/10.59531/ots.2025.3.2.115-144

Table 5. *Grain size fractions and resistivity ranges linked to permeability factors. [A szemcseméret frakciók és a fajlagos ellenállás tartományok hozzárendelése az áteresztőképesség faktorhoz.]*

Permeability factor	**Clay fraction [mm]**	**Silt fraction [mm]**	**Sand fraction [mm]**	**Gravel fraction [mm]**	**Resistivty range**
	0.00-0.005	0.005-0.06	0.06-2.0	2.0-40	Ohmm
0.8	72,9	22,4	3,9	0,5	<20
0.6	40,6	24,0	16,2	19,0	20-50
0.4	4,0	3,0	33,1	59,5	50-75
0.2	5,1	1,9	10,6	82,2	>75

https://doi.org/10.59531/ots.2025.3.2.115-144

***Figure 12**.: Grain size distribution of sediment samples compared with permeability factors and electrical resistivity values. [Fúrásminták szemcseméret eloszlásának összevetése a fajlagos ellenállással és az áteresztőképesség faktorral.]*

Vulnerability assessment

The vulnerability assessment of the investigated 3D site was not overly exciting, because being a dry, flat land, the slope and surface coverage factors didn't show any areal variation: f_1 took 0.8 and f_3 took 0.2. Consequently, as it was illustrated in Figure 9, the whole area is assessed to be very vulnerable to flooding from rain independently of the permeability factor f_2. Nevertheless, the high-resolution distribution of permeability may give help planning and implementing prevention and mitigation measures against pluvial flood.

For determination the permeability factor along the 3.2 km long survey line we

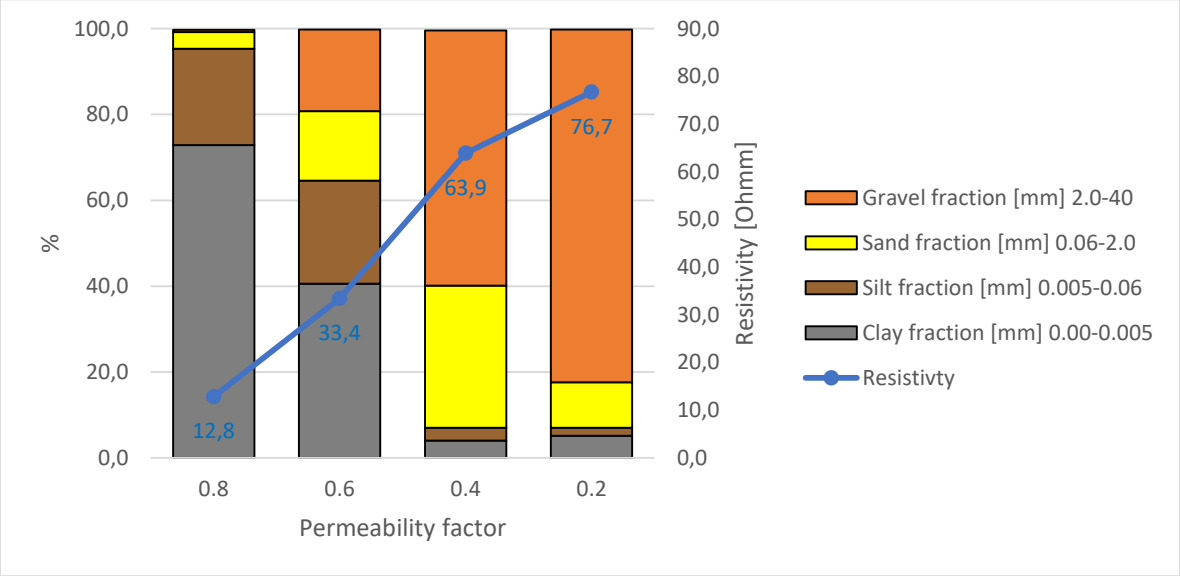

calculated the reference resistivity of the overburden: we took the median of the resistivity values in the depth range of 0-1.5 m in each horizontal reference point of the resistivity profile. Finally, we linked the median resistivity values to permeability factors according to Table 5. Figure 14 shows the fluctuations of the permeability factors as the function of median resistivity values and also its impact on the final vulnerability of the area.

https://doi.org/10.59531/ots.2025.3.2.115-144

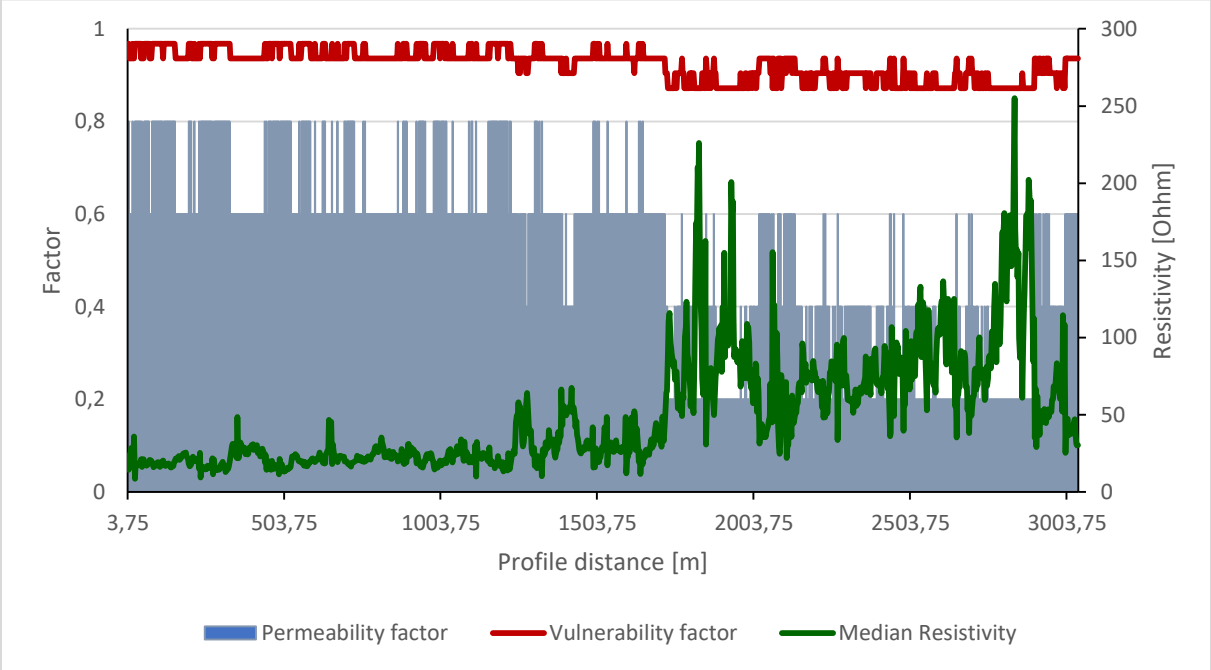

Figure 13. *Vulnerability and permeability factors of the 2D survey line calculated from the median resistivity values of the upper 1.5 m. [A 2D mérési vonal mentén a felső 1,5 m-re számított, sérülékenység és áteresztőképesség faktorok mediánértékei.]*

Discussion to Field study 2

In this field study we presented the process of vulnerability indexing using electrical resistivity data for qualifying the water permeability of the near-surface sections. For deriving the geological factor, we assigned the clay content of in situ soil samples to electrical resistivity. Since the area was quasi flat the distribution of the slope factor was uniform: the vulnerability index depended on only the clay content.

Results

In this study we demonstrated how geophysical methods can be used in indexing environmental vulnerability of sites that are endangered by pluvial floods.

The literature reports that vulnerability can be quantified using three factors: slope, drainage capacity and how much water covers the surface. We showed that once the joint impact of the three factors is calculated using the "probability or" operator, the vulnerability is always higher than the value of the highest factor.

https://doi.org/10.59531/ots.2025.3.2.115-144

Since the permeability factor is directly linked to the clay content, we worked out and tested methodologies applying shallow geophysical methods to determine clay content and thus permeability for indexing the environmental vulnerability. For pairing the physical parameters with geological ones, the geophysical surveying needs to be adjusted by analytics from drill hole samples, too.

For determination of permeability factors with GPR survey we introduced the parameter D_{10} that represents the attenuation of the high frequency electromagnetic wave due to the clay content of the layer. The application of the method was demonstrated in an urban area where the slope factor was determined from high resolution, digital terrain model.

In case of deriving permeability factor values with DC resistivity method, the electrical resistivity data were correlated with the variations of grain size distribution upon the laboratory analytics of drill hole samples.

Our filed tests showed that both the chosen geophysical methods are applicable for high resolution indexing environmental vulnerability in urban areas where pluvial flood is an environmental hazard.

Declaration of Interest

The authors declare that they have no known competitive financial interests or personal relationships that could have appeared to influence the work reported in this paper.

Acknowledgement

The field works of this study were financed by EAG grant from Iceland, Liechtenstein and Norway, project number: EEA-C11-1 (Field study 1) and the Mining and Geological Survey of Hungary (Field study 2).

REFERENCES

[1.] Boll J., van Rijn R.P.G., Weiler K.W., Ewen J.A., Daliparthy J., Herbert S.J. (1996): Using ground-penetrating radar to detect layers in a sandy field soil. – Geoderma, 70 (2-): 117–132. https://doi.org/10.1016/0016-7061(95)00077-1

[2.] Bruno Bueno, Leslie Norford, Grégoire Pigeon, Rex Britter (2012): A resistance-capacitance network model for the analysis of the interactions between the energy performance of buildings and the urban climate. – Building and Environment, 54, 116-125. https://doi.org/10.1016/j.buildenv.2012.01.023

[3.] Christensen, N.B. and Christiansen, A.V. (2021): Using geophysical survey results in the inference of aquifer vulnerability measures. – Near Surface Geophysics, 19: 505-521. https://doi.org/10.1002/nsg.12171

[4.] Dahlin, T. and Bernstone, C. (1997): A roll-along technique for 3D resistivity data acquisition with multi-electrode arrays. – In: Symposium on the Application of Geophysics to Engineering and Environmental Problems. 1997 January 927-935. https://doi.org/10.4133/1.2922474

[5.] Daniels, D. J., 2004. *Ground Penetrating Radar, 2nd Edition*. The Institute of Electrical Engineers, London, United Kingdom. https://doi.org/10.1049/PBRA015E

[6.] Dannowski, G. Yaramanci, U. (1999): Estimation of water content and porosity using combined radar and geoelectrical measurements. – European Journal of Environmental and Engineering Geophysics. 4 (1): 71-85.

[7.] Hou, J., Li, H., Zhu, H. and Wu, L. (2009): Determination of Clay Surface Potential: A More Reliable Approach. – Soil Sci. Soc. Am. J. 73 (5): 1658-1663. https://doi.org/10.2136/sssaj2008.0017

[8.] IPCC (2014): Summary for policymakers. – In: Climate Change 2014: Impacts, Adaptation and Vulnerability. Part A: Global and Sectoral Aspects. Contribution of Working Group II to Fifth Assessment Report of the Intergovernmental Panel on Climate Change.

[9.] Kalbfleisch J., G. (1985): Probability and statistical inference: volume 1: probability. – Springer, New York. https://doi.org/10.1007/978-1-4612-1096-2

[10.] Kirsch, R., Sengpiel, K.-P. and Voss, W. (2003): The use of electrical conductivity mapping in the definition of an aquifer vulnerability index. – Near Surface Geophysics, 1(1): 13-19. https://doi.org/10.3997/1873-0604.2002003

[11.] Loke M.H. and Barker, R.D. (1996): Rapid least-squares inversion of apparent resistivity pseudosections by a quasi-Newton method. – Geophysical Prospecting, 44 (1): 131-152. 04): Tutorial: 2-D and 3-D electrical imaging surveys.

[12.] Lunt I.A., Hubbard S.S. and Rubin Y. (2005): Soil moisture content estima-tion using ground-penetrating radar reflection data. – Journal of Hydrology, 307 (1-4): 254–269. https://doi.org/10.1016/j.jhydrol.2004.10.014

[13.] Neal A. (2004): Ground penetrating radar and its use in sedimentology: principles, problems and progress. – Earth-Science Reviews, 66 (3-4): 261–330. https://doi.org/10.1016/j.earscirev.2004.01.004

[14.] Plank, Z. and Polgár, D. (2019): Application of the DC resistivity method in urban geological problems of karstic areas. – Near Surface Geophysics, 17 (5): 547-561. https://doi.org/10.1002/nsg.12062

[15.] Plank, Z., Selmeczi, P., Pronay, Z., Polgar, D (2016): Geophysical Methods in Vulnerability Assessment to Climate Change Effect, We 22P1 16 https://doi.org 10.3997/2214-4609.201602063. Conference: Near Surface Geoscience 2016 - 22nd European Meeting of Environmental and Engineering Geophysics, Paper 1-5. https://doi.org10.3997/2214-4609.20142092

[16.] Obiora, D.N., Alhassan, U.D., Ibuot, J.C. and Okeke, F.N. (2016): Geoelectric Evaluation of Aquifer Potential and Vulnerability of Northern Paiko, Niger State, Nigeria. – Water Environment Research, 88 (7): 644-651. https://doi.org/10.2175/106143016X14609975746569

[17.] Rotárné Sz. Á., Selmeczi P., Homolya E. (2016): Ivóvízbázisok klímaváltozással szembeni sérülékenységének vizsgálati módszere [Method for assessing the vulnerability of drinking water resources to climate change]. – In: Tudásmegosztás, alkalmazkodás és éghajlatváltozás [Knowledge sharing, adaptation and climate change], Pálvölgyi T., Selmeczi Pál 8szerk.) MFGI, Budapest. pp 41-48.

[18.] Smith R. C., Sjogren D. B. (2006): An evaluation of electrical resistivity imaging (ERI) in Quaternary sediments, southern Alberta, Canada. – Geosphere. 2 (6): 287–298. https://doi.org 10.1130/GES00048.1

[19.] Słowik, M. (2014): Analysis of fluvial, lacustrine and anthropogenic landforms by means of ground-penetrating radar (GPR): field experiment. – Near Surface Geophysics, 12 (6): 777-792. https://doi.org/10.3997/1873-0604.2014033

[20.] Sperotto A.,Torresan S., Gallin V.,, Coppola E., Critto A.,Marcomini A. (2016): A multi-disciplinary approach to evaluate pluvial floods risk under changing climate: The case study of the municipality of Venice (Italy).– Science of The Total Environment, 562 (2016):1031-1043. https://doi.org/10.1016/j.scitotenv.2016.03.150

[21.] Steelman C.M. and Endres A.L. (2010): An examination of direct ground wave soil moisture monitoring over an annual cycle of soil conditions. – Water Resources Research 46, (11): W11533. https://doi.org/10.1029/2009WR008815

[22.] Wunderlich, T. and Rabbel, W. (2013): Absorption and frequency shift of GPR signals in sandy and silty soils: empirical relations between quality factor Q, complex permittivity and clay and water contents. – Near Surface Geophysics, 11 (2): 117-128. https://doi.org/10.3997/1873-0604.2012025

https://doi.org/10.59531/ots.2025.3.2.115-144

Absztrakt. A városi területek esőzések okozta villámárvíznek való kitettsége jellemezhető a környezeti sérülékenység indexszel. Ez a mérőszám három térbeli tényezőtől függ: a morfológiától, a felszínborítástól és a felszín vízáteresztő képességétől. Ez utóbbi tényezőt egyértelműen meghatározzák a felszín közeli rétegek összetétele és szerkezete, emiatt egyes geofizikai módszerek alkalmazása segíthet a vízelöntési veszélyeztetettség felmérésében. A publikáció bemutat egy módszertant, amit a környezeti sérülékenység nagy felbontású eloszlásának meghatározására dolgoztunk ki, két, városi környezetben is alkalmazható geofizikai felmérési módszer adatainak felhasználásával történik veszélyeztetettség minősítése. A talajradaros módszer esetében a felszíni vízáteresztő képességet a fedőréteg agyagtartalmához kötöttük, ezáltal az elektromágneses hullámok csillapodását, mint fizikai paramétert összefüggésbe hoztuk a környezeti sérülékenység vízáteresztési tényezőjével. A másik esetben ugyanezt a tényezőt az egyenáramú elektromos mérés adataiból határoztuk meg úgy, hogy a mérés során meghatározott, fajlagos elektromos ellenállás értéket a felső réteg domináns szemcseméret-eloszlásával hoztuk összefüggésbe. A kidolgozott módszertan alkalmazását két hazai városban végzet esettanulmányban mutatjuk be, ahol a környezeti sérülékenységet geofizikai szelvények mentén határoztuk meg az alkalmazott módszer által biztosított, vízszintes felbontással. Az első esettanulmányban a földradar módszert alkalmaztuk a vízáteresztési tényező meghatározására, és digitális terepmodell szolgált a lejtési adatok forrásaként. A második esettanulmány helyszíne egy sík terület volt, ahol nem volt szükség morfológiai adatokra. Az áteresztőképesség tényezőt egy három kilométer hosszú mérési vonalon mért, fajlagos ellenállás értékekből és a fúrásos talajminták szemcseméret-elemzési eredményeiből származtattuk.